
A First-Estimates Jacobian EKF for Improving SLAM Consistency

Guoquan P. Huang¹, Anastasios I. Mourikis^{1,2}, and Stergios I. Roumeliotis¹

¹Dept. of Computer Science and Engineering, University of Minnesota, Minneapolis, MN 55455

²Dept. of Electrical Engineering, University of California, Riverside, CA 92521

Email: {ghuang|mourikis|stergios}@cs.umn.edu

Summary. In this work, we study the inconsistency of EKF-based SLAM from the perspective of observability. We analytically prove that when the Jacobians of the system and measurement models are evaluated at the latest state estimates during every time step, the linearized error-state system employed in the EKF has observable subspace of dimension higher than that of the actual, nonlinear, SLAM system. As a result, the covariance estimates of the EKF undergo reduction in directions of the state space where no information is available, which is a primary cause of the inconsistency. Furthermore, a new “First-Estimates Jacobian” (FEJ) EKF is proposed to improve the estimator’s consistency during SLAM. The proposed algorithm performs better in terms of consistency, because when the filter Jacobians are calculated using the first-ever available estimates for each state variable, the error-state system model has an observable subspace of the same dimension as the underlying nonlinear SLAM system. The theoretical analysis is validated through both simulations and experiments.

1 Introduction

For autonomous vehicles exploring unknown environments, the ability to perform simultaneous localization and mapping (SLAM) is essential. Among the numerous algorithms developed thus far for the SLAM problem, the extended Kalman filter (EKF) remains one of the most popular ones, and has been used in several practical applications. In this work, we address the *consistency* issue of the EKF-SLAM algorithm, which has recently received considerable attention [1, 2, 3, 4, 5, 6]. As defined in [7], a state estimator is consistent if the estimation errors (i) are zero-mean, and (ii) have covariance matrix smaller or equal to the one calculated by the filter. Consistency is one of the primary criteria for evaluating the performance of any estimator; if an estimator is inconsistent, then the accuracy of the produced state estimates is unknown, which in turn makes the estimator unreliable.

In particular for the *standard* EKF-SLAM algorithm, there exists significant empirical evidence showing that the computed state estimates tend to be inconsistent. The first work to draw attention to this issue was that of Julier and Uhlmann [1], who observed that when a stationary robot observes a new landmark multiple times, the estimated variance of the robot’s orientation becomes smaller. Since the observation of a previously unseen feature does not provide any information about the robot’s state, this reduction is “artificial,” and leads to inconsistency. Bailey *et al.* [4] examined several symptoms of the inconsistency of the standard EKF algorithm, and argued, based on simulation results, that the uncertainty in the robot orientation is the main cause of the inconsistency of EKF-SLAM. The work of [5, 6] further confirmed the empirical findings in [4] and extended the analysis of [1] to the case of a robot that observes a landmark from *two* positions. It was shown that, in this special case, the violation of a certain condition that needs to be satisfied by the filter Jacobians leads to inconsistency.

The aforementioned works have described several symptoms of inconsistency that appear in the standard EKF-SLAM. However, they have not conducted a detailed analysis into the exact cause of inconsistency, for the general case of a moving robot. In this paper, we revisit the inconsistency problem from a new perspective, i.e., by analyzing the observability properties of the filter’s error-state system model. The main contributions of this work are the following:

- Through an observability analysis, we prove that the standard EKF-SLAM employs an error-state system model that has an unobservable subspace of dimension 2, even though the underlying nonlinear system model has 3 unobservable degrees of freedom (corresponding to the position and orientation of the global frame). This is a primary cause of inconsistency.
- We propose a new algorithm, termed *First Estimates Jacobian* (FEJ)-EKF, which improves the estimator’s consistency during SLAM. Specifically, we show analytically that when the EKF Jacobians are computed using the first-ever available estimates for each of the state variables, the error-state model has the *same* observability properties as the underlying nonlinear model. As a result of these properties, the new FEJ-EKF outperforms alternative approaches [3] in terms of accuracy and consistency.

2 SLAM Observability Analysis

It is well known that the propagation and measurement models for 2-D SLAM are generally nonlinear. In particular, the SLAM system is described by the following nonlinear process and measurement equations:

$$\mathbf{x}_{k+1} = \mathbf{f}(\mathbf{x}_k, \mathbf{w}_k) \tag{1}$$

$$\mathbf{z}_k = \mathbf{h}(\mathbf{x}_k) + \mathbf{n}_k \tag{2}$$

where \mathbf{x}_k is the state vector comprising the robot pose and landmark positions, \mathbf{w}_k is the process noise vector (i.e., the odometric noise), and \mathbf{n}_k is the exteroceptive measurement noise vector. The observability properties of this nonlinear system have been studied in the past [8], and it has been shown that the system is unobservable, with 3 unobservable degrees of freedom. This result agrees with intuition, which dictates that, since in SLAM only *relative* measurements between the robot and landmark are available, the *global* position and orientation of the state vector cannot be determined.

However, it should be noted that the EKF does not directly use the nonlinear model of (1)-(2). Instead, EKF-SLAM relies on the following linearized error-state propagation and measurement-residual equations, respectively:

$$\tilde{\mathbf{x}}_{k+1|k} \simeq \Phi_k \tilde{\mathbf{x}}_{k|k} + \mathbf{G}_k \mathbf{w}_k \quad (3)$$

$$\mathbf{r}_k \simeq \mathbf{H}_k \tilde{\mathbf{x}}_{k|k-1} + \mathbf{n}_k \quad (4)$$

where $\tilde{\mathbf{x}}_{\ell|j}$ is the error in the estimate of the state \mathbf{x}_ℓ , given all measurements up to time-step j . The Jacobian matrices Φ_k , \mathbf{G}_k , and \mathbf{H}_k are defined as:

$$\Phi_k = \nabla_{\mathbf{x}_k} \mathbf{f} \Big|_{\{\mathbf{x}_k^*, \mathbf{0}\}} \quad \mathbf{G}_k = \nabla_{\mathbf{w}_k} \mathbf{f} \Big|_{\{\mathbf{x}_k^*, \mathbf{0}\}} \quad \mathbf{H}_k = \nabla_{\mathbf{x}_k} \mathbf{h} \Big|_{\mathbf{x}_k^*} \quad (5)$$

In these expressions, \mathbf{x}_k^* denotes the *linearization point* for the state \mathbf{x}_k , used for evaluating the Jacobians, while a linearization point equal to the zero vector is chosen for the noise. The EKF employs the above linearized system model for propagating and updating the estimates of the state and covariance matrix, and thus the observability properties of this model affect the performance of the estimator. To the best of our knowledge, a study of these properties has not been carried out in the past, and is one of the main contributions of this work.

Since the linearized error-state model for EKF-SLAM is time-varying, we employ the *local observability matrix* [9] to perform the observability analysis. Specifically, the local observability matrix for the time interval between time-steps k and $k+m$ is defined as:

$$\mathbf{M} \triangleq \begin{bmatrix} \mathbf{H}_k \\ \mathbf{H}_{k+1} \Phi_k \\ \vdots \\ \mathbf{H}_{k+m} \Phi_{k+m-1} \cdots \Phi_k \end{bmatrix} = \mathbf{M}(\mathbf{x}_k^*, \mathbf{x}_{k+1}^*, \dots, \mathbf{x}_{k+m}^*) \quad (6)$$

This expression makes explicit the fact that the observability matrix is a function of the linearization points used in computing all the Jacobians within the time interval $[k, k+m]$. In turn, this implies that *the choice of linearization points affects the observability properties* of the linearized error-state system of the EKF. This key fact is the basis of our analysis. In the following, we discuss three possible choices for linearization, and the observability properties of the corresponding linearized systems. We note that, due to space limitations, the derivations have been omitted, and the interested reader is referred to [10] for details.

2.1 Ideal EKF-SLAM

We first examine the observability properties of the linearized system whose Jacobians are evaluated using the *true* values of the state. Clearly, this is an “oracle”, or “ideal” EKF, which is not realizable in practice. Considering the special structure of the Jacobian matrices, in [10] we prove that in this case the observability matrix is singular and has a nullspace of dimension three:

$$\dim(\text{Null}(\mathbf{M}_{\text{ideal}})) = 3 \quad (7)$$

Moreover, it is shown that the unobservable subspace of the system model in the ideal EKF is *identical* to the nullspace of the observability matrix of the underlying, nonlinear SLAM system [10]. This indicates that, if it were possible to evaluate the Jacobians using the true state values, the observability properties of the EKF system model would match those of the actual nonlinear system.

2.2 Standard EKF-SLAM

In a real-world implementation the true values of the state are not known, and thus it is not possible to employ them in computing the filter Jacobians. Instead, in the standard approach the *latest* state estimates are used in evaluating the Jacobians. In [10], we show that in this case, the unobservable subspace of the error-state model is only of dimension two:

$$\dim(\text{Null}(\mathbf{M}_{\text{std}})) = 2 \quad (8)$$

We thus see that the linearized error-state model employed in the standard EKF-SLAM has different observability properties than the ideal EKF-SLAM and the underlying nonlinear system. In particular, by processing measurements collected during the interval $[k, k + m]$, the EKF acquires information in all but two of the directions of the state space. However, this is incorrect, since the measurements in SLAM do not provide information about the global position and orientation of the state vector, which correspond to *three* degrees of freedom. In [10], it is shown that the direction “missing” from the unobservable subspace of the EKF system model is the one corresponding to the global orientation. Therefore, the filter gains “nonexistent” information about the robot’s global orientation. This leads to an unjustified reduction in the orientation uncertainty, which in turn, further reduces the uncertainty in all the state variables, causing inconsistency.

2.3 First-Estimates Jacobian EKF SLAM

Careful examination of the structure of the local observability matrix \mathbf{M} reveals that it is possible to obtain an EKF system model with an unobservable subspace of dimension 3, even if the Jacobians are not evaluated at the true

state values. In particular, this is possible with the following two modifications: (i) In the computation of the state-propagation Jacobian matrix Φ_k , we employ the propagated robot position estimate, $\hat{\mathbf{p}}_{R_{k|k-1}}$, instead of the updated one, $\hat{\mathbf{p}}_{R_{k|k}}$, and (ii) In the evaluation of the measurement Jacobian matrices we always utilize the landmark position estimate *from the first time* it was detected. As a result of these changes, the observability matrix \mathbf{M}_{FEJ} of this new filter, which we term *First-Estimates Jacobian* (FEJ)-EKF, has a nullspace of dimension three [10]:

$$\dim(\text{Null}(\mathbf{M}_{\text{FEJ}})) = 3 \quad (9)$$

This means that the number of unobservable directions in this new filter, which is *realizable in practice*, matches that of the underlying nonlinear system. Interestingly, even though the filter does not use the latest available state estimates (and thus utilizes Jacobians that are less accurate than those of the standard EKF), it exhibits better consistency properties than the standard EKF, as shown in the following section. This indicates that the observability properties of the EKF error-state model are fundamental in determining the consistency properties of the filter.

3 Results

In order to validate the preceding theoretical analysis and to demonstrate the capability of the FEJ-EKF filter to improve the consistency of EKF-SLAM, a series of Monte Carlo simulation tests and an experiment on a real-world data set were conducted. The metrics used to evaluate filter performance are: (i) the RMS error, and (ii) the average normalized (state) estimation error squared (NEES) [7]. Specifically, for the landmarks we compute the average RMS and average NEES errors by averaging the squared errors and the NEES, respectively, over all Monte Carlo runs, all landmarks and all time steps. On the other hand, for the robot pose we compute these error metrics by averaging over all Monte Carlo runs for each time step (cf. [10] for a more detailed description).

3.1 Simulation

In the simulation tests presented in this section, the robot moves at a constant velocity of $v = 0.25$ m/sec, the standard deviation of the velocity measurement noise is equal to $\sigma_v = 0.1v$, while the rotational velocity measurements are corrupted by noise with standard deviation $\sigma_\omega = 1^\circ/\text{sec}$. The robot records measurements of the relative position of landmarks that lie within its sensing range of 5 m, with standard deviation equal to 15% of the robot-to-landmark distance along each axis. It should be pointed out that the sensor-noise levels selected for the simulations are larger than what is typically encountered in

practice. This was done since larger noise levels lead to higher estimation errors, which in turn cause the Jacobian estimates to be less accurate, and make the effects of inconsistency more apparent.

In particular, a SLAM scenario with loop closure was considered where 100 Monte Carlo simulations were performed. During each run, the robot executes 10 loops on a circular trajectory, and observes 20 landmarks in total. Four filters process the same data, to ensure a fair comparison: (i) the ideal EKF, (ii) the standard EKF, (iii) the FEJ-EKF, and (iv) the robocentric filter [2, 3], which aims at improving the consistency of SLAM by expressing the landmarks in a robot-relative frame. The comparative results for all filters

Ideal EKF	Std EKF	FEJ-EKF	[2]
Robot Position Err. RMS (m)			
0.69	0.98	0.70	0.75
Robot Heading Err. RMS (rad)			
0.079	0.11	0.082	0.082
Robot Pose NEES			
3.05	12.79	3.68	6.70
Landmark Position Err. RMS (m)			
0.95	2.08	0.98	1.16
Landmark Position NEES			
2.1	12.93	2.35	6.65

Table 1. Robot Pose and Landmark Position Estimation Performance

are presented in Fig. 1 and Table 1. Specifically, Fig. 1(a) and Fig. 1(b) show the average NEES and RMS errors for the robot pose, respectively. On the other hand, Table 1 presents the average values of all relevant performance metrics for the landmarks and robot.

Several interesting conclusions can be drawn from these results. First, it becomes clear that the performance of the FEJ-EKF is *very close* to that of the ideal EKF, and substantially better than the standard EKF, both in terms of RMS errors and NEES. This occurs even though the Jacobians used in the FEJ-EKF are less accurate than those used in the standard EKF, as explained in the preceding section. This fact indicates that the errors introduced by the use of inaccurate Jacobians have a less detrimental effect on consistency than the use of an error-state system model with observable subspace of dimension larger than that of the actual, nonlinear, SLAM system.

A second observation is that the FEJ-EKF also performs much better than robocentric mapping [2], both in terms of accuracy and in terms of consistency. One possible justification for this is that in robocentric mapping, during each propagation step *all* landmark position estimates need to be reevaluated, since they are expressed with respect to the moving robot frame. As a result, during

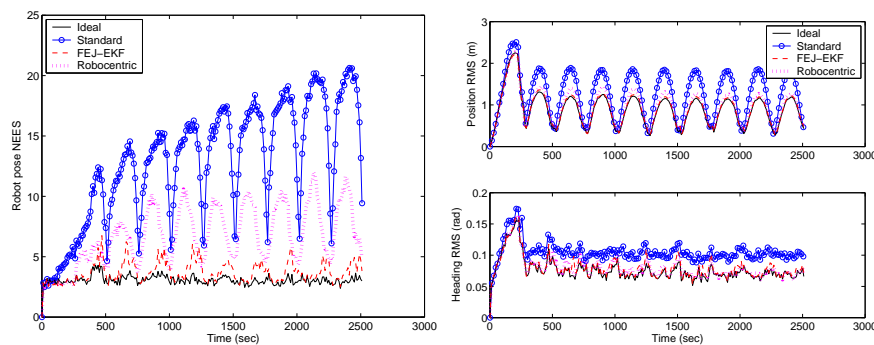


Fig. 1. Monte Carlo results for a SLAM scenario with multiple loop closures. (a) Average NEES of the robot pose errors (b) RMS errors for the robot pose (position and orientation). In these plots, the solid lines correspond to the ideal EKF, the dashed lines to the FEJ-EKF, the solid lines with circles to the standard EKF, and the dotted lines to the robocentric mapping algorithm of [2]. Note that the RMS errors of the ideal EKF and the FEJ-EKF are almost identical, which makes the corresponding lines difficult to distinguish.

each propagation step (termed *composition* in [2]), all landmark estimates and their covariance are affected by the linearization errors of the process model. This problem does not exist in the world-centric formulation of SLAM, and it could offer an explanation for the observed behavior. As a final remark, we note that even though the FEJ-EKF NEES performance is significantly better compared to that of the robocentric mapping, the difference in the RMS errors of the two filters is less pronounced. This indicates that the effects of inconsistency primarily affect the covariance, rather than the state estimates.

3.2 Experiment

To experimentally validate the performance of the FEJ-EKF, the filter was tested on the Sydney Car Park data set collected by Guivant and Nebot¹. The experimental platform is a 4-wheeled vehicle equipped with a GPS, a laser sensor, and wheel encoders. The kinematic GPS system was used to provide ground truth for the robot position with 5 cm accuracy. Since the GPS has different frequency (up to 2 Hz) from the other exteroceptive sensors, we interpolated the GPS data to obtain the ground truth at each time step. Wheel encoders were used to provide odometric measurements, and propagation was carried out using the Ackerman model. In this particular application, artificial landmarks were used that consisted of 60 mm steel poles covered with reflective tape. With this approach, it is easy to extract the features and the measurement model also becomes very accurate. Since the true position of

¹ The data set is available at: www-personal.acfr.usyd.edu.au/nebot/dataset

Std EKF	FEJ-EKF	[2]
Robot Position Err. RMS (m)		
0.1002	0.0523	0.0838
Robot Position NEES		
2.8900	2.5197	2.8265
Landmark Position Err. RMS (m)		
0.3812	0.1858	0.2755
Landmark Position NEES		
2.5196	2.0197	2.4800

Table 2. Robot and Landmark Position Estimation Performance

the landmarks was also obtained with GPS, a true map was available for comparison purposes.

In this test, because the ground truth for the robot orientation was still unavailable, the ideal EKF could not be tested, and therefore the following three filters were compared: (i) the standard EKF, (ii) the FEJ-EKF, and (iii) the robocentric mapping filter [2]. The comparison results are shown in Table 2 and Figs. 2 and 3. Specifically, Table 2 presents the average values of all relevant performance metrics for the robot and the landmarks. On the other hand, Fig. 2 shows the trajectory and landmark estimates produced by the three filters, while Fig. 3 shows the NEES and RMS errors of the robot position over time. We point out that the NEES in this case pertains only to the robot position, and therefore the “optimal” value for it is 2.

These results demonstrate that the performance of the FEJ-EKF is better than the standard EKF and the robocentric mapping filter, both in terms of consistency and in terms of accuracy. In particular, the average RMS and the average NEES for the FEJ-EKF are better than the corresponding ones for the two competing filters. These results, along with those of the simulations presented in the previous section, lead us to the conjecture that the mismatch in the dimension of the unobservable subspace between the linearized SLAM system and the underlying nonlinear system is a fundamental cause of filter inconsistency.

4 Conclusions

In this paper, we study the issue of filter inconsistency in EKF-based SLAM. By comparing the observability properties of the nonlinear SLAM system model with those of the linearized error-state model employed in the EKF, we proved that the observable subspace of the standard EKF is always of higher dimension than the observable subspace of the underlying nonlinear system. As a result, the covariance estimates of the EKF undergo reduction

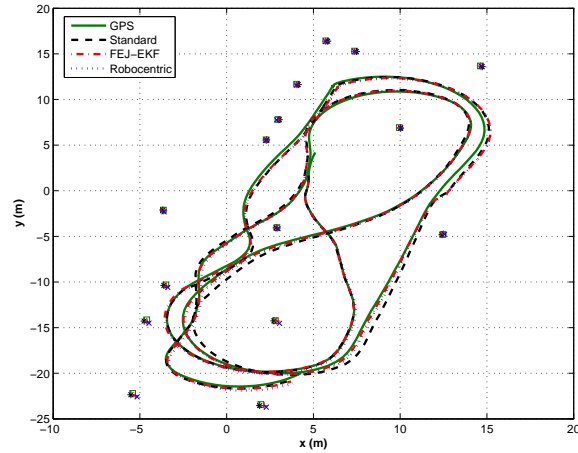


Fig. 2. The robot trajectory and landmark estimates. In this plot, the solid lines are ground truth obtained from GPS, while the boxes (\square) are the known beacon positions. On the other hand, the dashed lines and crosses (+) are the estimated trajectory and landmarks corresponding to the standard EKF, the dash-dotted lines and stars (*) correspond to the FEJ-EKF, and the dotted lines and x-crosses (\times) to the robocentric mapping [2].

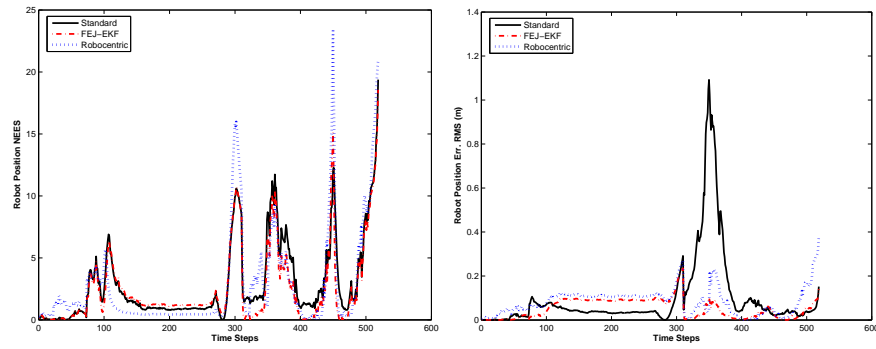


Fig. 3. (a) NEES of the robot position errors (b) RMS errors for the robot position. In these plots, the solid lines correspond to the standard EKF, the dash-dotted lines to the FEJ-EKF, and the dotted lines to the robocentric mapping algorithm of [2].

in directions of the state space where no information is available, which is a primary cause of inconsistency.

Based on this analysis, a new “First Estimates Jacobian” (FEJ) EKF is proposed to improve the estimator’s consistency during SLAM. The FEJ-EKF SLAM algorithm performs better with respect to consistency, because when the filter Jacobians are calculated using the first available estimate for each state variable, the error-state system model has an observable subspace

of the same dimension as the underlying nonlinear SLAM system. Through Monte Carlo simulations and experiments, we have verified that the FEJ-EKF is more accurate and more consistent than both the standard EKF and the robocentric mapping [2], which has been proposed for improving estimator consistency in SLAM.

Acknowledgements

This work was supported by the University of Minnesota (DTC), and the National Science Foundation (EIA-0324864, IIS-0643680, and IIS-0811946). Anastasios Mourikis was supported by the UMN Doctoral Dissertation Fellowship.

References

1. S. Julier and J. Uhlmann. A counter example to the theory of simultaneous localization and map building. In *IEEE International Conference on Robotics and Automation*, pages 4238–4243, Seoul, Korea, May 2001.
2. J.A. Castellanos, J. Neira, and J. Tardos. Limits to the consistency of EKF-based SLAM. In *5th IFAC Symposium on Intelligent Autonomous Vehicles*, pages 1244–1249, Lisbon, Portugal, July 2004.
3. J.A. Castellanos, R. Martinez-Cantin, J. Tardos, and J. Neira. Robocentric map joining: Improving the consistency of EKF-SLAM. *Robotics and Autonomous Systems*, 55(1):21–29, January 2007.
4. T. Bailey, J. Nieto, J. Guivant, M. Stevens, and E. Nebot. Consistency of the EKF-SLAM algorithm. In *IEEE/RSJ International Conference on Intelligent Robots and Systems*, pages 3562–3568, Beijing, China, Oct. 2006.
5. S. Huang and G. Dissanayake. Convergence analysis for extended Kalman filter based SLAM. In *IEEE International Conference on Robotics and Automation (ICRA)*.
6. S. Huang and G. Dissanayake. Convergence and consistency analysis for extended Kalman filter based SLAM. *IEEE Transactions on Robotics*, 23(5):1036–1049, Oct. 2007.
7. Y. Bar-Shalom, X.R. Li, and T. Kirubarajan. *Estimation with applications to tracking and navigation*. New York: Wiley, 2001.
8. K.W. Lee, W.S. Wijesoma, and J.I. Guzman. On the observability and observability analysis of SLAM. In *IEEE/RSJ International Conference on Intelligent Robots and Systems (IROS)*, pages 3569–3574, Beijing, China, Oct. 2006.
9. Z. Chen, K. Jiang, and J.C. Hung. Local observability matrix and its application to observability analyses. In *16th Annual Conference of IEEE (IECON'90)*, pages 100–103, Pacific Grove, CA, Nov. 1990.
10. G. Huang, A. Mourikis, and S. Roumeliotis. Generalized analysis and improvement of the consistency for EKF-based SLAM. Technical report, University of Minnesota, Minneapolis, MN, January 2008. www.cs.umn.edu/~ghuang/paper/TR_slam_genconsistency.pdf.